Effect of Dynamic Strain Aging on Fracture in Aluminum Alloy Sheet Materials AA5754

J. Kang,[1] D.S. Wilkinson,[1] A.J. Beaudoin,[2] J.D. Embury,[1] Raja K. Mishra [3]
[1] *McMaster University, Hamilton, Ontario, Canada*
[2] *University of Illinois at Urbana-Champaign, Urbana, Illinois, U.S.A.*
[3] *General Motors R&D Center, Warren, MI, U.S.A.*

E-mail: *kangjd@mcmaster.ca*

Abstract

Solid-solution alloys such as Al-Mg alloy AA5754 often display serrated flow during tensile deformation due to dynamic strain aging over a range of temperatures and strain rates. The effect of dynamic strain aging on fracture properties has been an important concern in addition to surface quality and formability. In this paper, we present the results for double-edge-notched samples tested at room temperature. Digital image correlation was utilized to follow the deformation pattern during the tensile processes. The results show that the plasticity bursts are not limited to the notch tip causing the plastic zone to be finger-like. This cannot be predicted using conventional elastic-plastic fracture models. The results show that the fracture strain increases with increasing strain rate. We have also used 45 degree offset-edge notched samples also tested at room temperature. The results here show that the ductile crack propagates along the original crack line leading to the final failure.

Introduction

It is well known that for solid solution alloys such as the Al-Mg system, serrated flow occurs over a wide range of temperature and strain rate. In Al-Mg alloys this phenomenon is referred to as the Portevin-Le Chatelier (PLC) effect. It is commonly accepted that the PLC effect is caused by dynamic strain aging associated with the interaction of solute atoms (Mg) with moving dislocations [1]. The serrated stress-strain response of the material leads to band-type macroscopic surface markings. These limit the potential application of the material by degrading surface quality. There has been intensive study of the PLC effect in Al-Mg alloys including both experimental investigations and numerical modeling [1-5].

Research on the effect of dynamic strain aging on fracture in the presence of a stress concentration has been very limited but also controversial [6-10]. Theoretical predictions suggest that the PLC effect should be beneficial in brittle materials but detrimental in more ductile materials [6-7]. However, Delafosse et al [8] found tearing resistance in an Al-Li 2091 alloy is maximized in the temperature range concurrent with dynamic strain aging. In addition, Graff et al

[9] emphasize the heterogeneous propagation of localized bands within a general plastic zone of notched and cracked specimens.

The present study focuses on the effect of dynamic strain aging on the distribution of plastic deformation in a strip cast AA5754 automotive aluminum sheet in the presence of notches. Uniaxial tensile, double edge notched and offset notched samples have been tested. The digital image correlation method was used to follow the deformation patterns under various conditions.

Experimental

The materials used in the present study were made from continuous cast AA5754 slabs, rolled to a 1 mm gauge and put in an O-temper . The nominal chemical composition is 3.42 wt.% Mg, 0.23 wt.% Mn, 0.05 wt.% Si, 0.08 wt.% Fe, and the balance being Al.

Tensile tests were performed at room temperature using an Instron 5566 screw-driven tensile machine at strain rates of 6×10^{-4}/s, 6×10^{-3}/s and 6×10^{-2}/s. Type-B Portevin-Le Chatelier bands were evident under uniaxial tension at a strain rate of 6×10^{-4}/s. In order to assess the PLC effect more quantitatively, we have then used double-edge notched samples to concentrate the initiation of PLC bands at a known location. In some of the samples the notches were placed on opposite sides (a/w=0.2), while in others they were offset by 45 degrees (Fig. 1). All notched samples were tested at the same nominal strain rates at room temperature as those in uniaxial (unnotched) tensile tests.

Full-field strain mapping based on digital image correlation was used to follow the plastic deformation processes occurring during the tensile tests [10]. A commercially available DIC system, named Aramis, was used for this purpose. A calibration procedure was established, which ensured that the measuring error in strain is distributed randomly with a maximum error less than 0.25% over a range of in-plane displacement from –3 mm to 3 mm and out of plane displacement from –0.6 mm to 0.6 mm [11-13].

All of the samples with or without notches were examined after rupture. The fracture surface areas were measured using stereo-optical microscopy in order to calculate the true fracture strain $\varepsilon_f = \ln(\frac{A_o}{A_f})$.

Results and discussion

Elastic fracture mechanics analysis based on the von Mises yield criterion [14], has shown that the plastic zone ahead of a crack tip in Mode I has a “kidney” shape under plane stress condition (Fig. 2). This shows that plastic deformation is concentrated only in vicinity of the crack tip and preferentially at 45 degrees to the tensile axis.

However, the cumulative strain mapping measurements shown in Fig. 3 for a notched specimen show that PLC bands run across the width of the specimen and spread out from the crack tip in a wide zone with an angle of approximately 30 degrees. The movie created from the time evolution of the DIC images clearly shows both continuous and hopping propagation of the bands. Furthermore, it is evident from Fig. 3 that plasticity bursts occur in areas well removed from the stress concentration (in this case, the crack tip). The strain pattern in the vicinity of crack tips shows “horizontal” or “finger type” character. This feature is found for all the strain rates tested in this study (Fig. 4). Note that all samples fractured along line connecting the notches for all three strain rates tested here.

Since plasticity is not limited to the notch tip in these samples but rather spreads over the sample, it is reasonable to postulate that the PLC bands might affect the crack propagation path. In order to investigate this, the two edge notches were offset 45 degrees to provide a favorite path for the PLC bands. It is interesting to notice that at small applied strain (Fig. 5(a)), plastic strain is concentrated in vicinity of each notch tip and develops separately for each notch. When the applied strain increases, PLC bands are seen moving between the two notches (Fig. 5(b)). As deformation proceeds a horizontal feature starts to appear ahead of the notch tip. However, the evolving PLC bands eventually do not change the crack propagation path; instead, each crack propagates along its own crack line until fracture (Fig. 5(c) and (d)).

Recalling Fig. 2, it is evident that the salient features of plasticity at a stress concentrator in 5xxx aluminum alloys cannot be predicted using classic elastic plastic fracture analysis. Instead one needs to incorporate dynamic strain aging effects. Indeed, a recent finite element analysis by Mach et al [15, 16] based on crystal plasticity using a constitutive equation that includes dynamic strain aging has successfully revealed all these features.
Fractured samples from both the uniaxial tensile tests and double edge notched tensile tests were used to calculate true fracture strains, based on area reduction. The results show that the fracture strains fall on a single trend line and that the fracture strain increases with strain rate for both notched and un-notched samples (Fig. 6).

Conclusions

The effect of dynamic strain aging on fracture properties has been studied for an AA5754 sheet materials using digital image correlation. The results show that the plasticity bursts are not limited to the notch tip leading to the horizontal feature of the plastic zone. This cannot be predicted using conventional elastic-plastic fracture models. The measured fracture strain show that the fracture strain increases with increasing strain rate. Samples with notches offset at 45 degree show that the ductile crack propagates along the original crack line leading to the final failure.

References

[1] J D Baird, Dynamic strain aging, in The Inhomogeneity of Plastic Deformation, ASM, Metal Park, Ohio, 191-222, 1973.
[2] M Li and D J Lege. J. Eng. Mater. Technol. 120, 48-56,1998.[3] L P Kubin, K Chihab and Y Estrin. Acta metall. 36, 2707-2718 (1988).
[4] P G McCormick. Acta metall. 19, 463-471 (1971).
[5] L P Kubin and Y Estrin. Journal de Physique III, 1(6):929–943, 1991.
[6] Y Brechet and F Louchet. Acta Metall. Mater., 41(3):783–791, 1993.
[7] F Louchet and Y Brechet. Acta Metall. Mater., 41(3):793–800, 1993.
[8] D Delafosse, G Lapasset, and L P Kubin. Scripta Metall. Mater., 29:1379–1384, 1993.
[9] S Graff, S Forest, J-L Strudel, C Prioul, P Pilvin, and J-L B´echade. Scripta Mater., 52:1181–1186, 2005.
[10] Aramis v4.7 manual, GOM mbH, Braunschweig, Germany (2001).
[11] J Kang, D S Wilkinson, J D Embury, M Jain, and A J Beaudoin. Scripta Mater., 53:499–503, 2005.
[12] J Kang, D S Wilkinson, M Jain, J D Embury, A J Beaudoin, S Kim, R Mishra, and A K Sachdev. Acta Mater., 54:209–218, 2006.
[13] J Kang, D S Wilkinson, M Bruhis, M Jain, P D Wu, J D Embury, R K Mishra, A K Sachdev. Journal of Materials Engineering and Performance, 17(3):395-401.
[14] T L Anderson, Fracture mechanics: fundamentals and applications. CRC Press, Boca Raton, Florida, 80, 1995.
[15] J C Mach, J Kang, A J Beaudoin, D S Wilkinson. Materials Science Forum Vols. 519-521 (2006) pp. 85-92.
[16] J C Mach, Numerical simulation of dynamic strain aging and fracture in aluminum, M.S. thesis, UIUC, Urbana, Illinois, U.S.A., 2004.

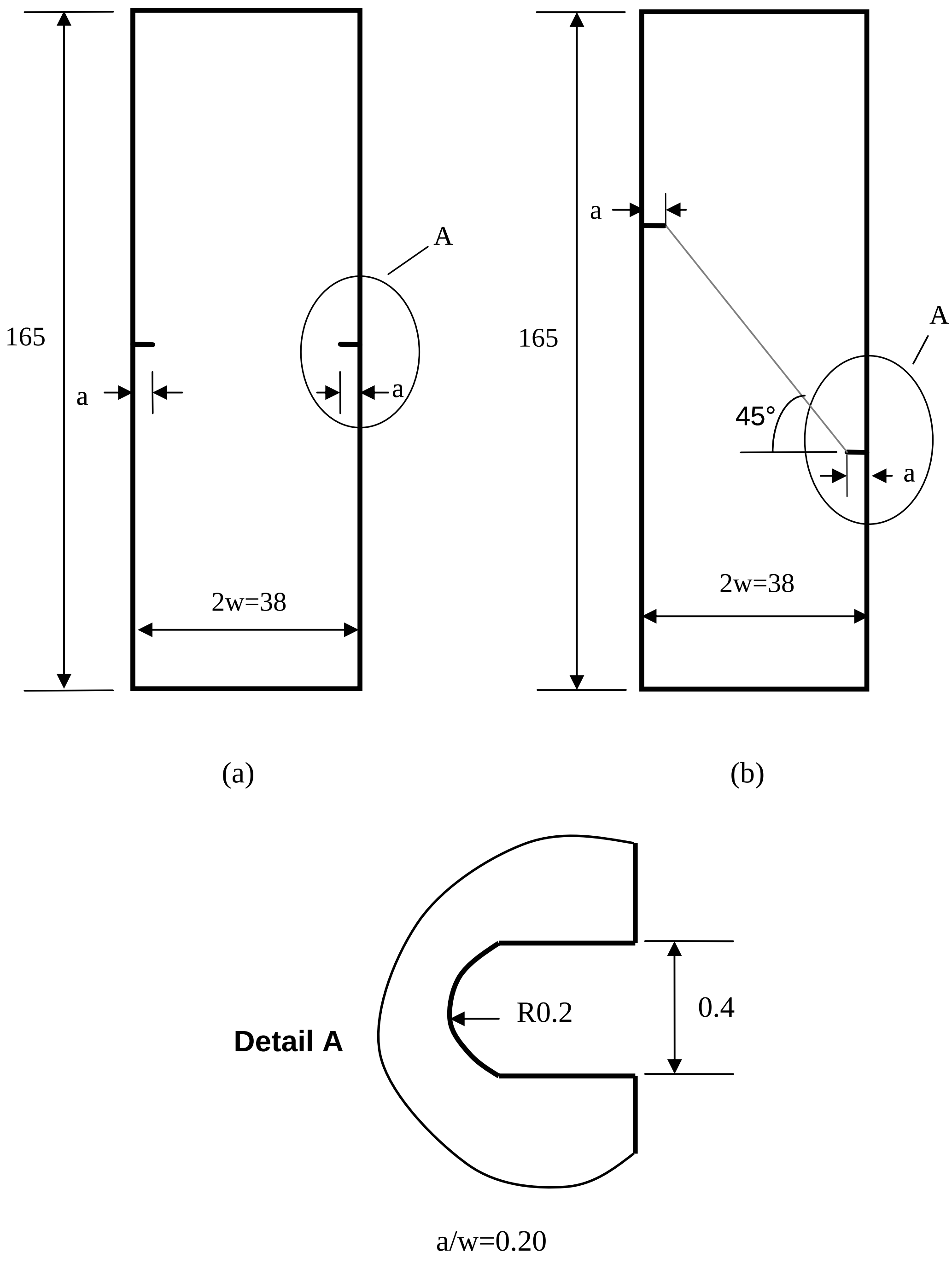

Fig.1 Schematic of (a) double edge notched and (b) offset edge notched samples.

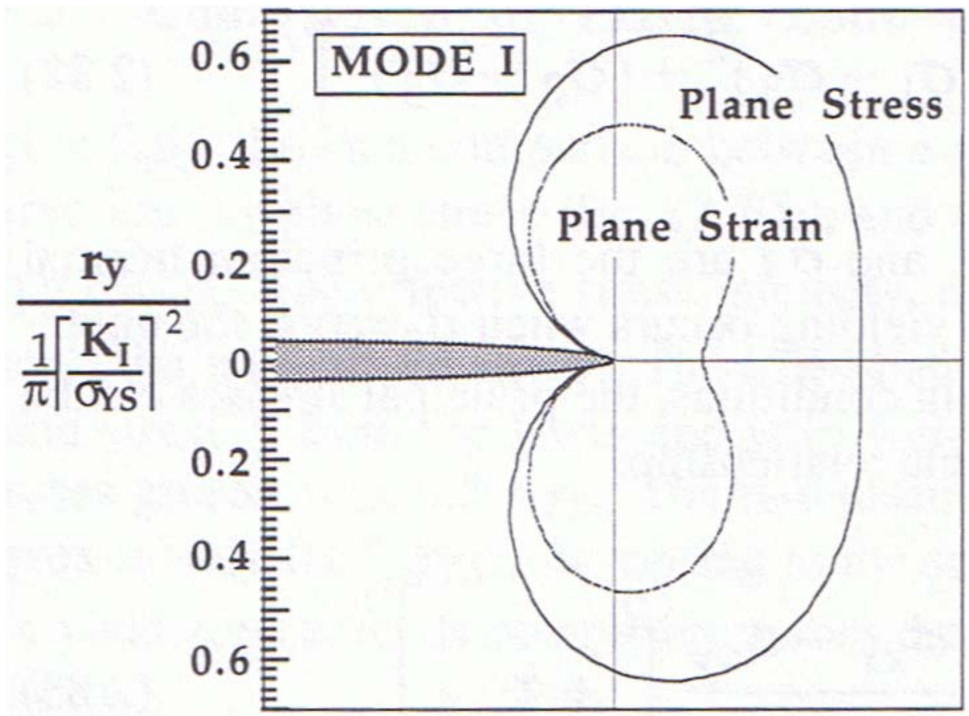

Fig. 2 Crack tip plastic zone shapes in Mode I estimated from the elastic solutions and von Mises yield criterion [14].

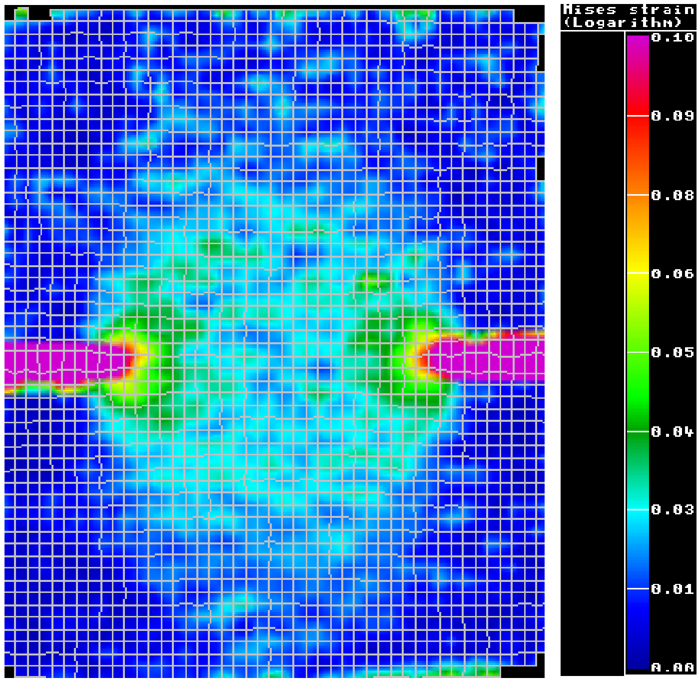

(a) Global strain: 0.01

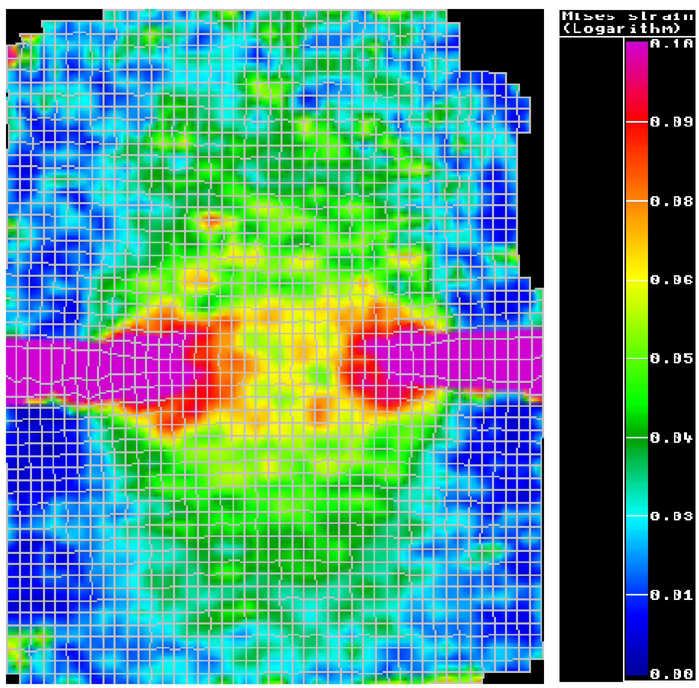

(b) Global strain: 0.025

Fig. 3 Effective strain distribution in double edge notched samples with a/w=0.20, 2w=38mm.

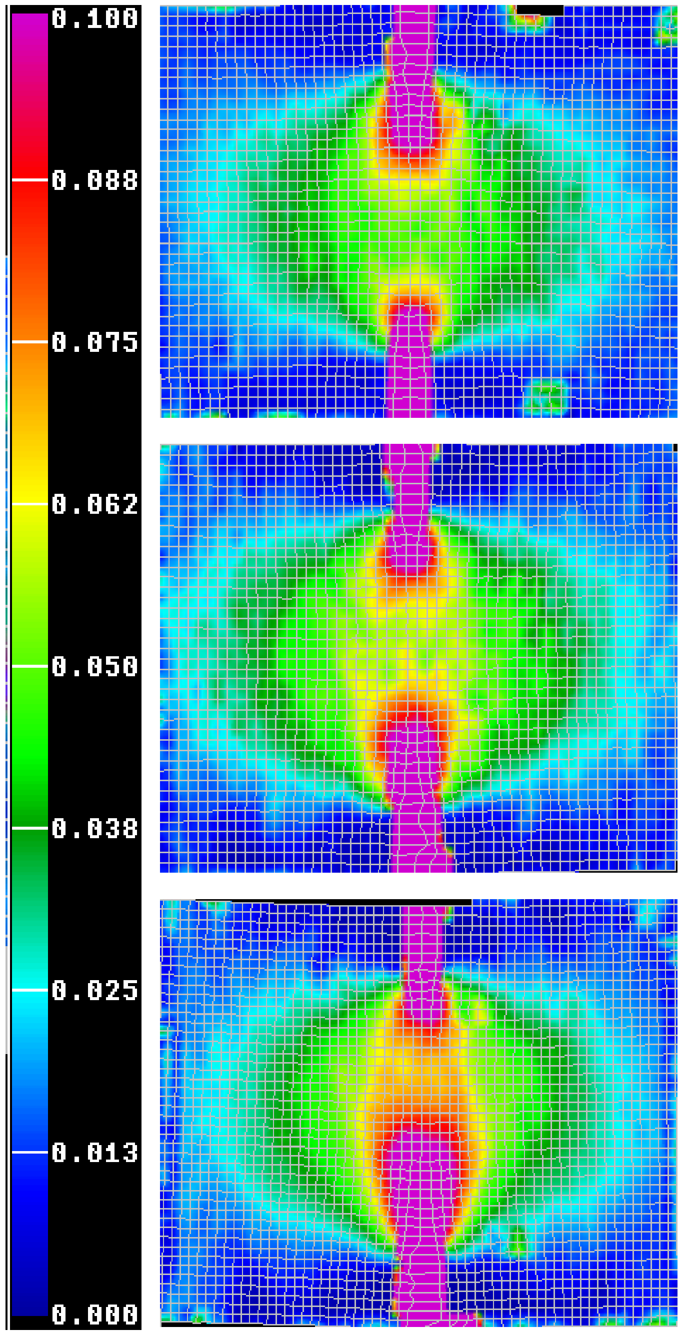

(a) strain rate: 6×10^{-4}/s

(b) strain rate: 6×10^{-3}/s

(c) strain rate: 6×10^{-2}/s

Fig. 4 Effective strain distribution at maximum load under three different strain rate for double edge notched samples with a/w=0.20, 2w=38 mm [12].

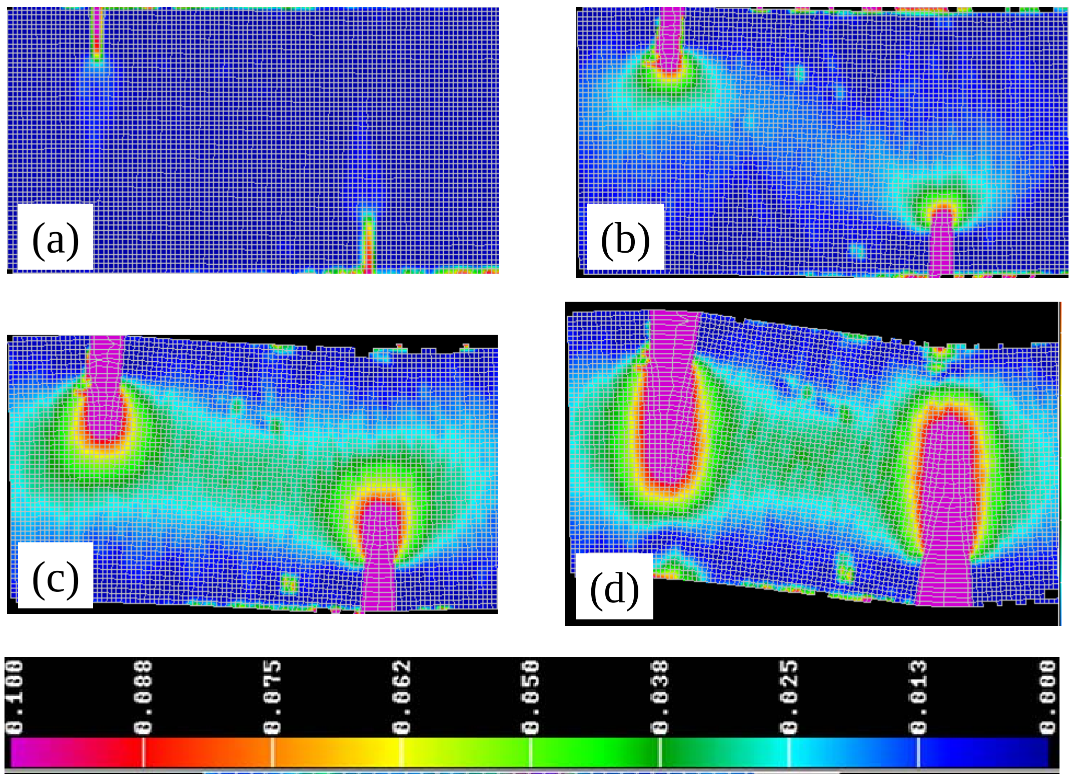

Fig. 5 Effective strain distribution in offset edge notched samples.

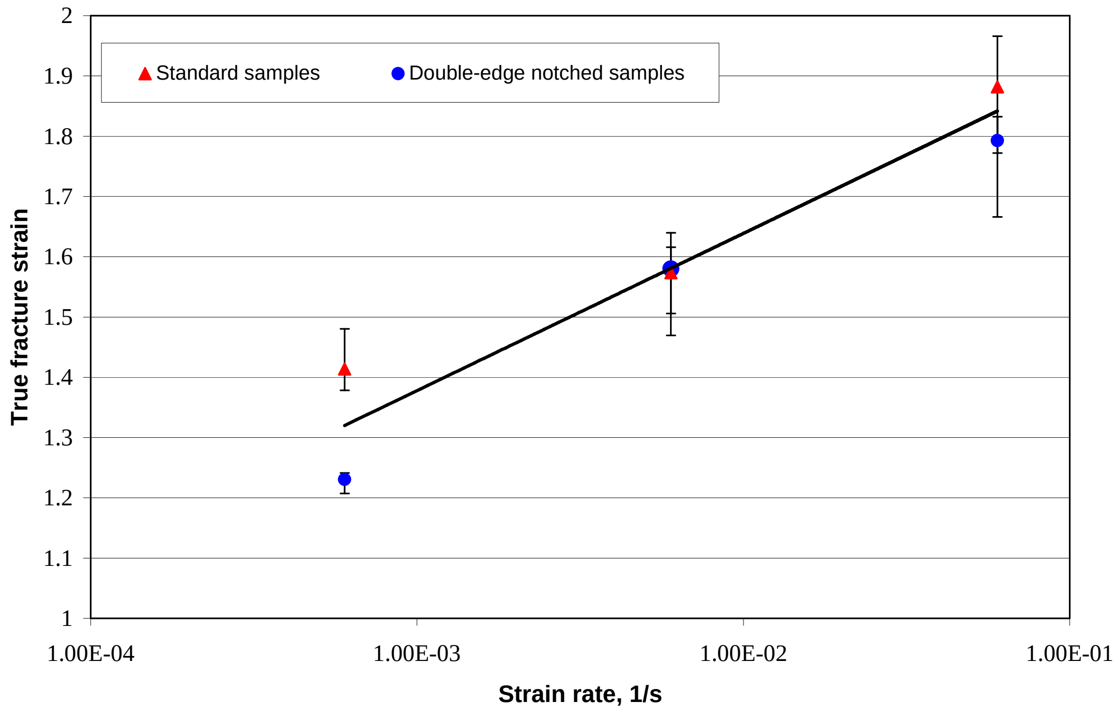

Fig. 6 Fracture strains at different strain rate with and without notches. Y-error bars represent the maximum and minimum values of fracture strains in the corresponding measurements [12].